JOURNAL OF MATERIALS SCIENCE 18 (1983) 1095–1118

The performance and causes of failure of polyethylene pipes subjected to constant and fluctuating internal pressure loadings

M. B. BARKER*, J. BOWMAN, M. BEVIS
Department of Non-Metallic Materials, Brunel University, Uxbridge, Middlesex, UK

Three different pipe-grade polyethylenes, in the form of one large and three small diameter pipe systems, have been tested at elevated temperatures, using constant and fluctuating internal pressure loadings that resulted in brittle fractures. The behaviour under fatigue of two of the three types of small diameter polyethylene pipes was substantially described by a cumulative damage model, whilst the third exhibited a fatigue weakness, an observation not previously reported. The performance of the large diameter pipes under fatigue was dominated by the presence of large voids in the pipe wall that arose from incorrect processing and resulted in premature failure. The sites of crack initiation in one material grade of the small diameter systems were examined in detail. In particular the size, position and composition of particles initiating fracture were determined. The maximum particle size on the fracture surface of the pipe was found to correlate reasonably well with a measure of pipe lifetime, as predicted by a fracture mechanics approach, and indicated that the lifetime of this one type of polyethylene pipe was dependent on the size of the inclusions initiating fracture.

1. Introduction

Low (LDPE), medium (MDPE) and high (HDPE) density polyethylenes are routinely processed into pipe and fittings for pressure pipeline systems that find ready application in the gas, water and chemical process industries. The available design data for these systems is basically in the form of stress-rupture curves [1], which identify the lifetimes of pipes loaded under static internal pressures at fixed and well defined temperatures. However, plastics pipeline systems are composed not only of extruded pipe, but normally also of injection moulded fittings and of joints made between pipe and pipe, and pipe and fittings. Further, the system in operation may be subjected to fluctuating internal pressure loadings in addition to static pressures [2]. Therefore, in order to characterize fully system performance, in respect of internal pressure loadings, it is perspicacious to examine the performance of the pipe, the fittings and the joints together under both static and fluctuating internal pressures. This paper presents the results of part of such a programme and reports the performance and causes of failure of medium and high density polyethylene pipe tested at elevated temperatures under constant and fluctuating internal pressures. The present results therefore provide information on the performance of pipe which is to be compared, in subsequent publications [3], to the performance of pipe systems incorporating injection moulded fittings, mirror-plate butt welds and spigot and socket joints, loaded under constant and fluctuating internal pressure loadings.

Three different non-crosslinked polyethylene materials, designed specifically for pipe applications, have been tested as one large and three small diameter pipe systems. The three resins,

*Present address: Associated Octel Co. Ltd., Oil Sites Road, Ellesmere Port, Cheshire.

0022–2461/83 $03.00 + .12

labelled PE1, PE2 and PE3 included both MDPE and HDPE with the material density within the range 935 to 965 kg m^{-3}. Pipes were supplied "off the shelf", and the density, crystalline melting temperature, and melt index of material cut from the pipes were determined and found to be within the material manufacturer's specification.

In detail the work on these four pipe systems can be divided into three areas:

(a) Small, 60 or 63 mm, diameter SDR11 (SDR, Standard Dimension Ratio, is the outside diameter of the pipe divided by its wall thickness) pipes extruded from the three PE resins, were tested without end restraint at 80° C under constant and fluctuating internal pressures to give brittle fractures. (Subsequently constant pressure will be termed stress-rupture testing although the names creep and static fatigue [4] are sometimes applied; fluctuating pressure tests will be referred to as fatigue, although the terms dynamic fatigue and intermittant creep testing sometimes designate this mode of loading). Fatigue tests used a trapezoidal loading profile with the frequency within the range 0.8 to 7.5 cycles per minute (cpm) (0.014 to 0.125 Hz), with the internal pressure cycling between a set maximum and zero gauge pressure. The lifetimes of the pipes were recorded for the various internal pressures and loading profiles employed.

(b) Fracture surfaces from selected small diameter pipe failures were examined. Photographs characterized the fracture surface "macrostructure", while scanning electron microscopy (SEM) examined the shape, size and position of any particle initiating fracture. Energy dispersive X-ray analysis (EDX) techniques on the electron microscope identified the nature of the particle initiating fracture. Fracture surface shape is related to the loading profile, while the size and position of the particle initiating fracture is correlated with a measure of the pipe system lifetime.

(c) Finally, the performance of the PE1 material in the large (160 mm) diameter thick walled (SDR11) pipe form has been ascertained under fatigue loading at 6 cpm at 80° C. These tests are not as complete as the authors would wish; however, they are included as they illustrate the influence of voiding on pipe lifetimes.

2. Stress-rupture testing of polyethylene pipe

2.1. Modes of failure

There is general agreement within Europe that stress-rupture curves for HDPE and MDPE pipe contain a "knee", see Fig. 1. Above the knee the

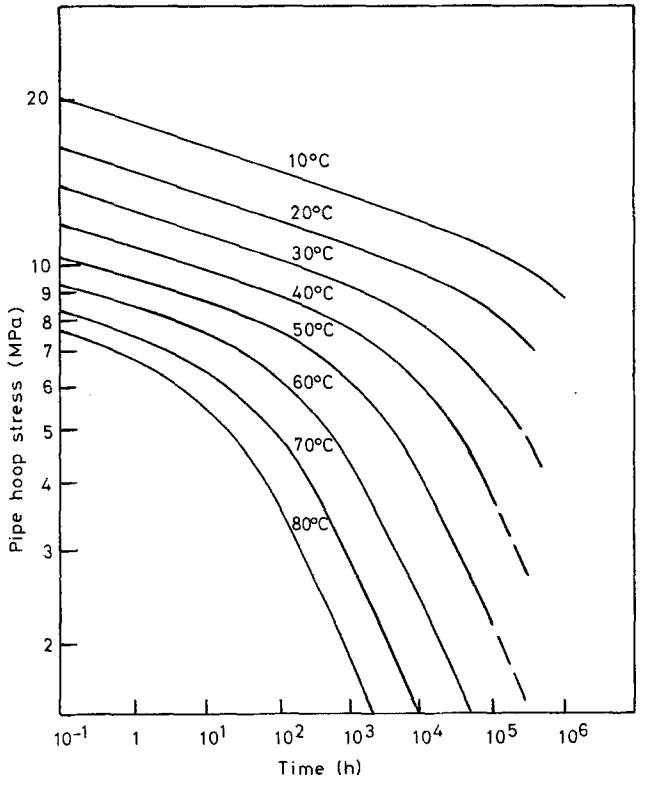

Figure 1 Stress-rupture curves typical of high and medium density polyethylene pressure pipe. The inital shallow incline of each curve gives way to a steeper section at longer times with the knee being the region where this change occurs.

material deforms in a gross ductile manner with a significant local straining of the material prior to failure, while below the knee a brittle crack propagates through the wall of the pipe with little or no evidence of ductility and only small hoop strains in the pipe [1, 5, 6]. Fig. 1 illustrates that for realistic design lifetimes the likely mode of failure is by the propagation of a brittle crack through the pipe wall. Experience shows that these cracks nucleate at or near the inside wall of the pipe, where the hoop stresses are greatest (see Appendix), and propagate through to the outside [7, 8]; the cracks lie parallel with the pipe extrusion direction and open in response to the larger stress, the hoop.

2.2. Theories of stress-rupture failure times

Two different approaches to calculate the lifetimes of plastics subject to a constant load or stress have been proposed, one based on the application of fracture mechanics [9] to slow stable crack growth, the other from the theory of activated rate processes developed by Eyring *et al.* [10] and applied to plastics pipes by Barton and Cherry [11]. The results presented later in the paper are best explained using a fracture mechanics approach.

Gray, Mallinson and Price [12] applied fracture mechanics to the case of slow stable crack growth in HDPE materials, and found the rate of crack growth, da/dt, could be given by

$$\frac{da}{dt} = BK_c^b \tag{1}$$

where B and b are material constants and K_c, the stress intensification at the tip of the growing crack, is given by

$$K_c^2 = Y^2\pi a\sigma^2 \tag{2}$$

where Y is a geometrical factor, σ is the applied stress and a is the crack length. If it is assumed that a plastics pipe, of wall thickness h, fails by the propagation of a brittle crack from a defect of size a_0 lying close to the pipe bore, then by substituting Equation 2 in Equation 1 and integrating between the limits a_0 and h, the lifetime of the pipe, τ_{SR} is given by Equation 3 below (Y is assumed to be approximately constant for the major part of the crack growth).

$$\tau_{SR} = \frac{2}{b-2}\left[a_0^{(1-b/2)} - h^{(1-b/2)}\right]\frac{(Y\sigma\pi^{1/2})^{-b}}{B} \tag{3}$$

If $h \gg a_0$ and b is not equal to 2, then the above equation may simplify to

$$\tau_{SR} = \left[\frac{2(Y\sigma\pi^{1/2})^{-b}}{B(b-2)}\right] \cdot a_0^{(1-b/2)} \tag{4}$$

where the terms in the square bracket are constant for testing at both a given fixed temperature and pipe hoop stress. The lifetime of the pipe, assuming that the material obeys Equation 1, is then dependent on the size of the defect initiating fracture.

For two unnotched HDPE pipes Gray *et al.* [12] demonstrated that Equation 3 described lifetimes by assuming defect sizes between 10 and 100 μm (these HDPE resins obeyed Equation 1). However, one of the newer pipe materials (i.e. BP Chemicals Ltd. Rigidex 002-40 MDPE) failed to obey Equation 1; Equations 3 and 4 could not therefore be applied to identify the influence of defect size on lifetimes of pipes processed from this material.

3. Fatigue of plastics

Plastics components subjected to fatigue may fail by one of at least three modes; fatigue thermal melting, cumulative damage due to stress, and crack propagation due to the repeated application of stress.

Failure by fatigue thermal melting is due to the hysteretic energy generated during each loading cycle [13–15] causing a rise in the temperature of the component which precipitates failure. High (> 10 Hz) loading frequencies, large stress ranges and low rates of cooling are usually required [15] to induce this mode of failure.

3.1. Cumulative damage model

The cumulative damage concept of fatigue failure assumes damage accumulates only during that time the part is subjected to stress, failure occurring when the accumulated damage reaches a critical value [16]. For simple loading profiles, such as a rectilinear wave form, the cumulative damage concept of fatigue failure can easily predict the number of cycles to failure, N_f, using an expression similar to that of Stapel [17, 18]:

$$N_f = \left[\frac{\tau_{SR}}{t_{max}}\right]_{T,\sigma} \tag{5}$$

where τ_{SR} is the stress-rupture lifetime and t_{max} is that time span in each cycle when the load is equal

to the set maximum. Equation 5 has no frequency dependence nor a restriction on t_{max}. Neither is there an allowance for damage recovery, so that it must be assumed that either the recovery or the time off load is negligible.

3.2. Cycle dependent failure

In cycle dependent failure the repeated application of stress, rather than the time for which the stress is applied, induces damage and causes a crack to propagate. The rate of crack propagation is in terms of the number of loading cycles, n, and is given most simply by [15, 19]

$$\frac{da}{dn} = D(\Delta K)^d \quad (6)$$

D and d are material constants, and ΔK, the stress intensity factor range, is given by

$$\Delta K^2 = Y^2 \pi a (\Delta\sigma)^2 \quad (7)$$

where Y and a are as in Equation 2 and $\Delta\sigma$ is the applied stress range. For plastics, the frequency of loading can have a considerable influence on both material constants (D and d) [15, 20]. Equations 6 and 7 may be integrated to give equations similar to Equations 3 and 4 but describing lifetime in terms of the number of cycles to failure, N_f, [21].

The experimental evidence which identifies the applicability of the above mentioned analysis of fracture to the pipe materials studied, is presented below.

4. Experimental details

4.1. Pipe sample dimensions

Stress-rupture and fatigue tests were conducted on the small diameter pipes using sample lengths of ten times the pipe outside diameter between end closures. Fatigue tests on the large diameter pipes used sample lengths in excess of one metre. Closure was effected by using either polypropylene end plugs retained by threaded caps screwed onto the pipe or welded on stub flanges with backing plates and retaining rings [22]. None of the pipe systems were end restrained during testing. Pipe systems were filled with tap water and tested, after conditioning, in a temperature controlled water bath at 79.5° C (± 0.5° C). Pressures for testing were selected to give brittle failures.

4.2. Stress-rupture testing

Stress-rupture tests on small diameter pipes were conducted according to ASTM D1598 by top loading the pipes with compressed air. Failure was detected by an electrical current detection technique [23]; electrodes were inserted in the water internal and external to the pipe and a potential sustained between the two so that when failure occurred a small current passed which identified failure, stopped a timer, isolated the failed system from the compressed air and released the pressure within the pipe system. A schematic presentation of the testing system for the generation of stress-rupture data is shown in Fig. 2a.

4.3. Fatigue testing

Fatigue tests on the small and large diameter pipes were conducted at frequencies between 0.86 and 7.5 cpm using a trapezoidal wave form of loading with a fixed pressure time-off of six seconds. Compressed air, top loading the systems, pressurised the samples. A three-way solenoid value, controlled by an electronic timer, directed the compressed air to and from the systems under test. When failure of a system occurred, the pipe failure detection unit (described above) activated the stop valve to isolate the system from the compressed air, see Fig. 2b. In all the fatigue tests reported here the internal pressure cycled between the set maximum and zero gauge; the stress ratio, $R (= \sigma_{min}/\sigma_{max})$, was therefore equal to zero. The rate of pressure build-up was constant for all frequencies of testing at any one set maximum pressure; for 1 MPa maximum internal pressure the rate of build-up was approximately 1 MPa sec^{-1}.

The pressure of the compressed air for stress-rupture and fatigue testing was tested using a linear displacement pressure transducer. Typical pressure profiles for low and high frequency fatigue tests are shown in Fig. 3. The time under maximum load, t_{max}, for any one loading cycle was computed using the time when the pressure of the gas within the system had attained 95% of the set value.

4.4. Fracture surface analysis

Failed pipes were cut to isolate and reveal the fracture surface, which was photographed and the ratio $2c/h$ determined, where h is the pipe wall thickness and $2c$ is the maximum extent of the brittle fracture along the pipe direction, see Fig. 4. Specimens were then coated with Au–Pd (care was taken to avoid local heating) and two features of the fracture surfaces were examined using a SEM.

First, the shape, size and position (with respect to the inside wall of the pipe) of any particle initiating fracture were ascertained and secondly, the elemental composition of these particles was determined using the EDX technique.

5. Experimental results

5.1. Measurement of the performance of plastics pipes

The performance of the plastics pipes subjected to constant and fluctuating internal pressure loading is presented in three ways.

First, as the time under maximum load. For stress-rupture testing this is simply τ_{SR}, while for fatigue the corresponding parameter is $\tau_{FATIGUE}$, given by

$$\tau_{FATIGUE} = \sum_{n=1}^{n=N_f} (t_{max})_n \qquad (8)$$

with t_{max}, n and N_f as described in Sections 3.2 and 4.3. $\tau_{FATIGUE}$ may be termed the pseudo stress-rupture lifetime, and is a concept previously utilized to allow comparisons to be made between stress-rupture and fatigue data [24]. The trapezoidal fatigue loading profile used in this study had a fixed rate of pressurization, implying a near constant rate of loading to reduce effects associated with rate of straining [9], and a fixed time-off load and hence recovery time. This form of loading profile should allow comparisons to be made between τ_{SR} and $\tau_{FATIGUE}$ at different frequencies, as only t_{max} is being varied. If $\tau_{SR} \approx \tau_{FATIGUE}$ at all frequencies, then for those testing conditions the plastics pipe exhibits no substantial weakness under fatigue. If, however, $\tau_{SR} \gg \tau_{FATIGUE}$, the reverse is true.

Secondly, pipe performance was defined by the total testing time, τ_{TEST}. Clearly, for stress-rupture testing, $\tau_{SR} = \tau_{TEST}$. For fatigue,

$$\tau_{TEST} = \sum_{n=1}^{n=N_f} (t_{cycle})_n \qquad (9)$$

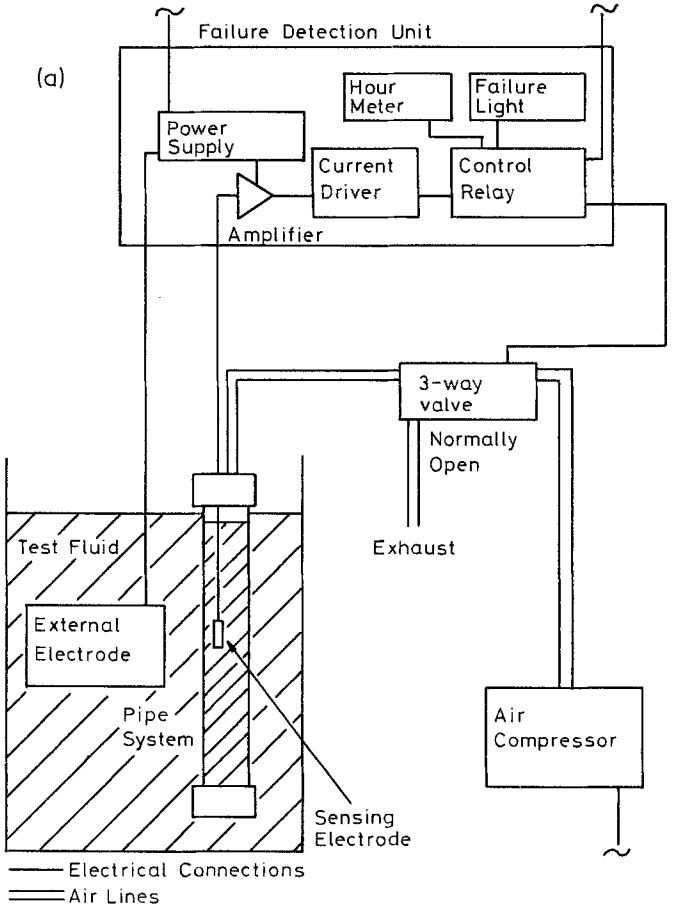

Figure 2 Schematic representation of the arrangements for pressurizing and detecting failure of the polyethylene pipe systems subjected to a constant (a) or an alternating (b) internal pressure loading.

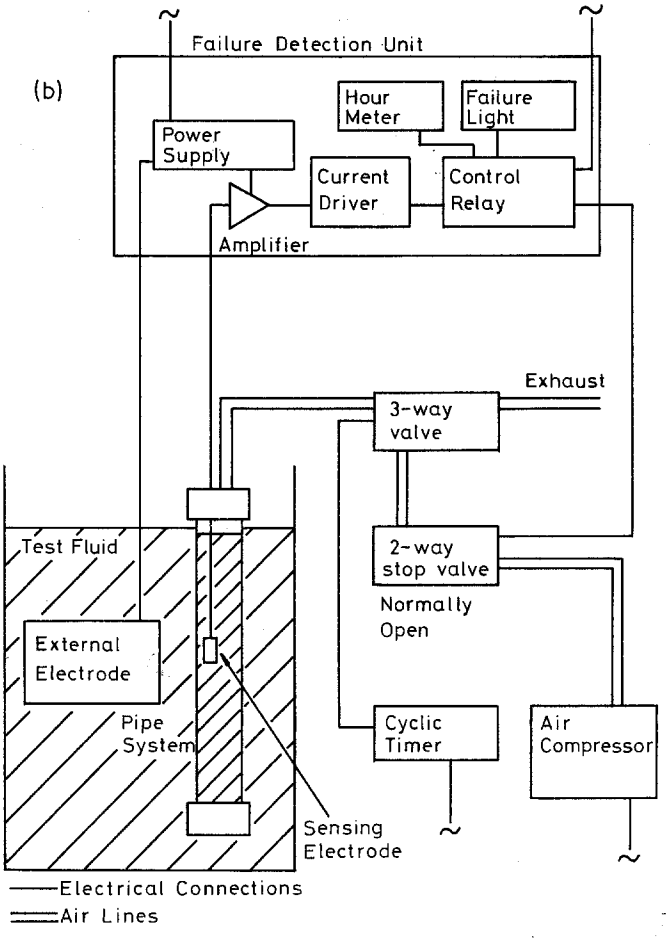

Figure 2 Continued.

where t_{cycle} is the time required for one complete loading cycle. Since t_{max} must be less than t_{cycle}, then $\tau_{TEST} > \tau_{FATIGUE}$, for fatigue loading. In addition, for a pipe loaded under fatigue τ_{TEST} may exceed τ_{SR} especially if the time-off load is large. In the field, it is τ_{TEST} that is recorded, rather than $\tau_{FATIGUE}$, although the latter is the more fundamental measure of pipe performance.

Thirdly, and finally, the performance of the plastics pipes loaded under fatigue is measured by the number of cycles to failure. The data for stress-rupture testing cannot meaningfully be presented here. Note that as the frequency is varied only the time under maximum load, t_{max}, is changing. Rate of pressurization and time-off load are both constant.

For simplicity the mean values for τ_{SR}, $\tau_{FATIGUE}$, τ_{TEST} and N_f are presented and plotted in Figs. 5, 6 and 7. The distribution of lifetimes was assumed normal and the sample standard deviation calculated and inserted to indicate the spread in the values of lifetimes. The authors note that for certain pipes the distribution of the stress-rupture lifetimes has been shown to be logarithmic-normal [1, 25]. Calculation of the sample standard deviation from the lifetime better indicates the range of values recorded.

5.2. Mechanical performance of the small diameter pipes

For all three small diameter PE pipes the influence of frequency of loading on pipe performance is shown in Figs. 5, 6 and 7. In Fig. 5 pipe performance is expressed by τ_{SR} and $\tau_{FATIGUE}$. All failures of pipe for the data in Fig. 5 were brittle, occurred at a distance greater than one pipe diameter from the end closure, and lay parallel with the extrusion direction. Increasing the frequency of loading (reducing t_{max}) in all cases reduced $\tau_{FATIGUE}$ below τ_{SR}. However, only for PE2 was $\tau_{FATIGUE}$ reduced substantially to indicate a potential fatigue weakness.

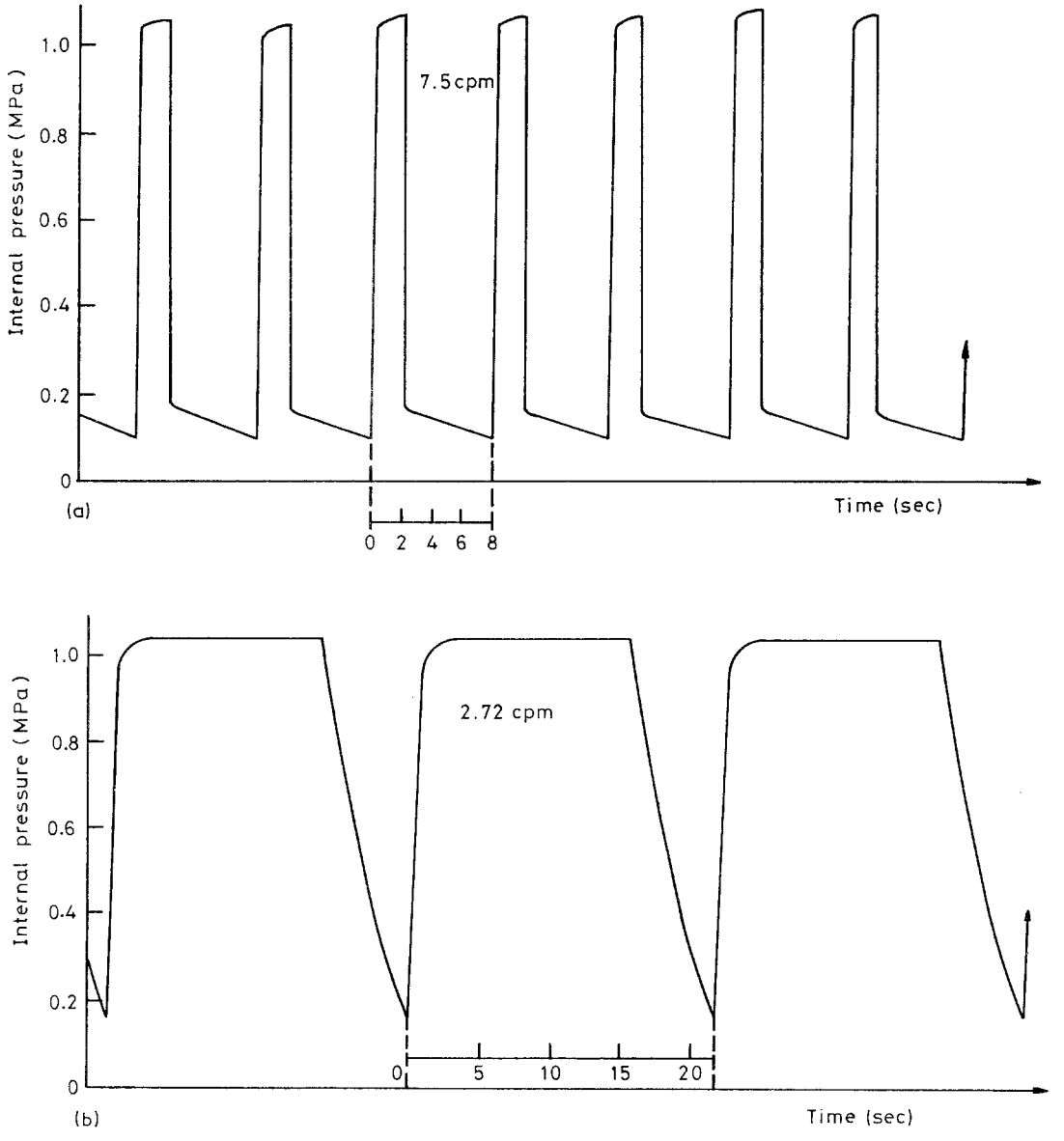

Figure 3 The recorded internal pressure variations in fatigue loaded pipe systems, using frequencies of 7.5 (a) and 2.72 cpm (b).

In Fig. 6 pipe performance is expressed by τ_{TEST}. Clearly, for a pipe which does not exhibit a marked fatigue weakness, testing under fatigue prolongs the time of the test substantially. If, however, the pipe does exhibit a fatigue weakness, τ_{TEST} can be reduced to a value below τ_{SR}, depending, of course, on the time-off load. This latter case was observed for the PE2 pipes.

In Fig. 7, as the frequency was increased, the number of cycles to failure for the PE1 and PE3 increased markedly. This behaviour is expected from the data presented for these pipes in Fig. 5, where $\tau_{FATIGUE}$ is of the same order as τ_{SR}, so that by reducing t_{max} (that is increasing the frequency of loading) N_f must be increased. For the PE2 pipes only one fatigue test was undertaken, due to the protracted testing time. However, a large number of samples were tested at this high frequency to confirm the weakness under fatigue.

5.3. Fracture surface characterization from small diameter pipes

5.3.1. Macro-features

Figs. 4a, b, c and d, e, f are photographs of fracture

surfaces from pipe stress-rupture and fatigue tested, respectively. They illustrate the overall features common to and characteristic of the two loading modes and the different polyethylene pipe materials.

For all pipe systems (all materials and both small and large diameter pipes) the overall shape of the fracture surface reflected the imposed loading mode. For fatigue loaded pipe systems the fracture tended to propagate preferentially along the pipe axis, Fig. 4, with increasing frequency of loading extending the fracture along the inside

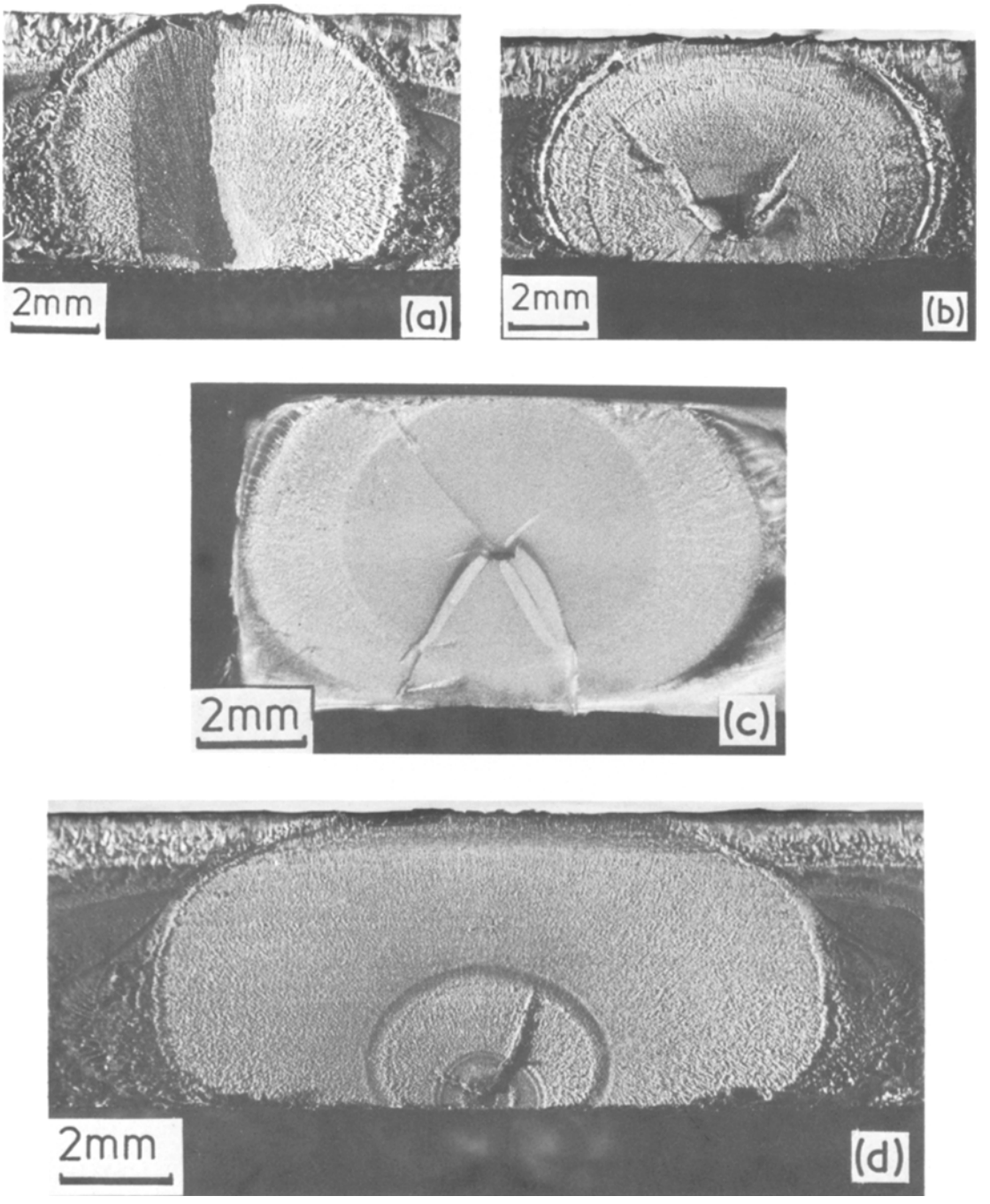

Figure 4 Low magnification optical photomicrographs of fracture surfaces from stress-rupture ((a), (b) and (c)) and fatigue ((d), (e) and (f)) tested pipe. PE1 pipe failures are (a) and (d), PE2 (b) and (e) and PE3 (c) and (f).

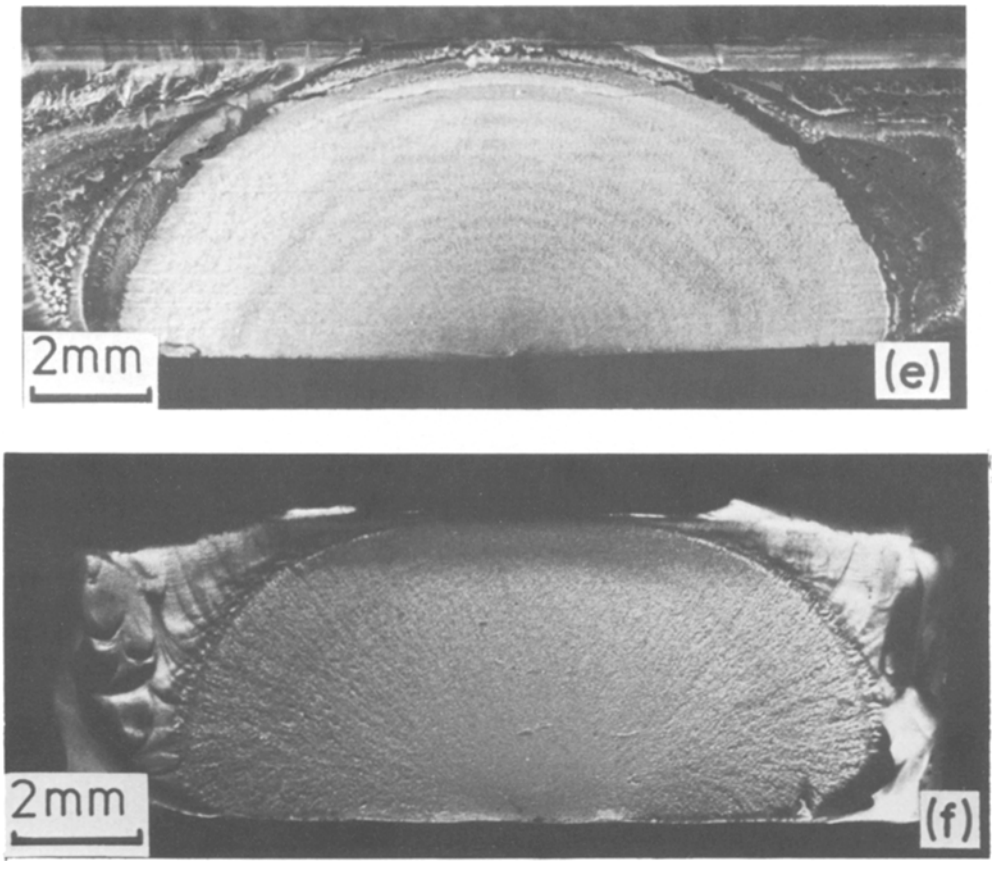

Figure 4 Continued.

wall of the pipe parallel with the pipe axis, Fig. 8. Fatigue loading is expected to introduce "beach markings" [15], but low magnification stereo light microscopy of PE1 and PE3 pipe fracture surfaces revealed no such markings. There were, however, clear beach markings on the fracture surfaces of the PE2 pipe fatigue tested and some evidence for pipe stress-rupture tested. For all pipe materials, but only on some fracture surfaces, was there evidence of the extrusion process used to manufacture the pipe. Lines running parallel with the extrusion direction were discernible for both stress-rupture and fatigue testing. In addition, lines in a radial direction, that is lying perpendicular to the crack growth front, emanate from the source of fracture in some cases, Fig. 4.

The site of fracture initiation appeared to be material and loading mode specific. In PE1 at both pressures under both loading modes, and in PE2 pipe under fatigue loading only, failure initiated at or near the inside wall of the pipe, Fig. 4. The few exceptions to this rule occurred where fracture was initiated by large or fibrous inclusions (only two failures in over a hundred tests initiated from this type of defect) which lay towards the centre of the pipe wall. In the limited number of stress-rupture tests undertaken on PE2 pipe, and in the PE3 pipe under both loading modes, failure was as likely to occur towards the middle of the pipe wall, Fig. 4.

5.3.2. Fracture initiation in PE1 pipes

Examination of fracture surfaces of stess-rupture and fatigue tested PE1 pipe revealed over 95% of failures clearly initiating from particles, examples of which are shown in Fig. 9. No failures in the small diameter pipes were observed to initiate from macro-voids (see Section 5.4). The distribution of the maximum extent, on the fracture surface, of the initiating particles is illustrated in Fig. 10a, which shows "particle size" predominantly below 700 μm. The majority of particles initiating fracture in the PE1 pipe lay close to the inside wall of the pipe, Fig. 10b.

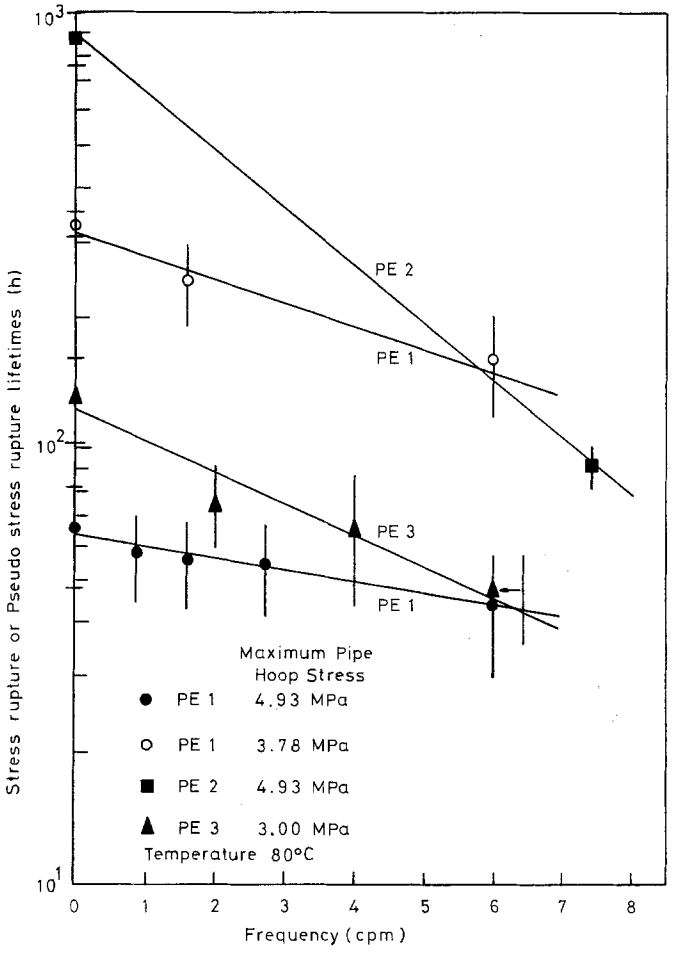

Figure 5 The stress-rupture (τ_{SR}) or pseudo stress-rupture ($\tau_{FATIGUE}$), (see Equation 8) lifetimes of the various polyethylene pipe systems as a function of frequency of loading. The bars indicate the standard deviation calculated from the lifetimes.

The elements present in the particle initiating fracture were investigated using the EDX technique. Pairs of EDX spectra, for the initiating particle and the same fracture surface but remote from the initiation site, are presented in Fig. 11. Lines due to palladium and gold are from the coating process. Three types of particle have been observed to initiate fracture in PE1 pipe, the calcium rich, the metallic and particles where no elements were detected: 52% initiated from particles where no elements could be detected, 16% from calcium rich and the remainder from iron or titanium based particles.

5.4. Mechanical performance of large diameter pipes

160 mm SDR11 pipe, produced from the same material (but not necessarily the same batch) as used for the small diameter PE1 pipe, was tested only under fatigue at a fixed loading frequency of 6 cpm (0.1 Hz), a maximum internal pressure of 1 MPa and at 80° C. Five failures were recorded, four of which initiated from macro-voids in the pipe wall, Fig. 12. The pseudo stress-rupture lifetimes of pipes failing from such defects were between 3 and 6 h (mean lifetime 4.8 h). The fifth failure initiated from a small particle, similar in size to those initiating fracture in the small diameter pipes. The pseudo stress-rupture lifetime for this failure was in excess of 50 h, a similar lifetime being recorded, for identical testing conditions, on the small diameter SDR11 PE1 pipes, Fig. 5.

6. Discussion

6.1. The mechanical performance of the small diameter pipes

The performance of the small diameter polyethylene pipes loaded under constant and fluctuating internal pressure loadings is described by τ_{SR} and $\tau_{FATIGUE}$, respectively. For testing at the same temperature and maximum hoop stress, Fig. 5

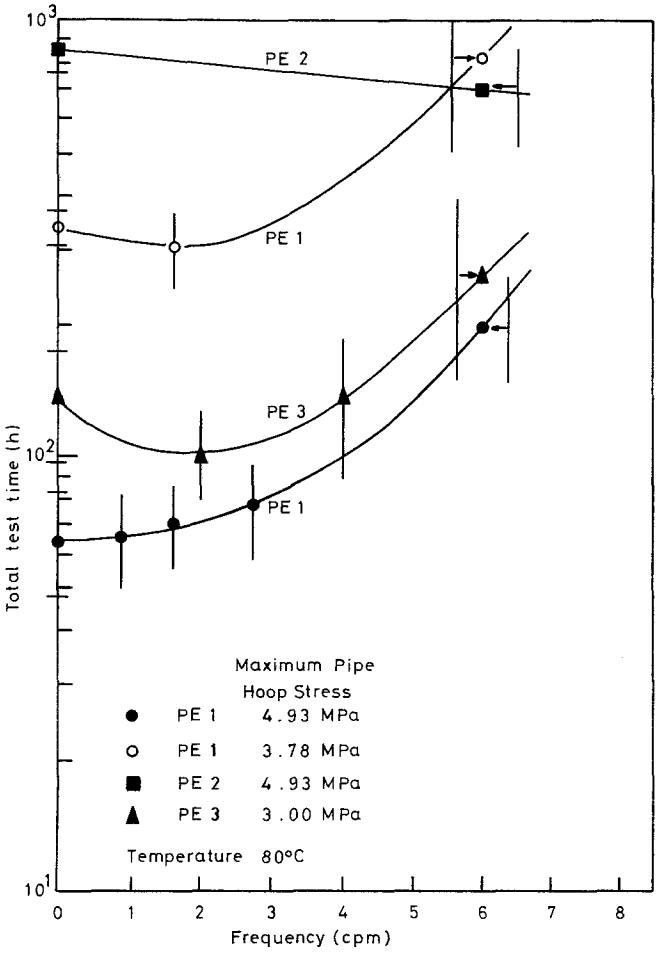

Figure 6 The total test time (τ_{TEST}, see Equation 9) as a function of loading frequency for the various polyethylene pipes.

shows that, when τ_{SR} is compared to $\tau_{FATIGUE}$, a clear distinction can be made between the PE2 and the PE1 and PE3 pipes. The PE2 pipes exhibited a pronounced fatigue weakness, not evident for the PE1 and PE3 pipes. The two cases are therefore discussed separately.

6.1.1. The fatigue performance of the PE1 and PE3 pipes

Neglecting fatigue thermal melting, which at these low loading frequencies (<0.2 Hz) and stresses is not observed, the failure of a plastics pipe subjected to a fluctuating internal pressure loading is due either to the accumulated damage from the stress acting, or from the action of applying the stress. If the pipe fails by the former mechanism, the use of trapezoidal loading profile allows a prediction of the number of cycles required to cause failure, by use of Equation 5 and the measured value of τ_{SR}. For the PE3 pipes and the PE1 pipes at both maximum internal pressures, a value of N_f, calculated via Equation 5, is compared with the experimental results and presented in Fig. 13.

Considering first the performance of the PE1 pipe at the higher stress; Figs. 5, 7 and 13 allow the following conclusions to be drawn:

(a) $\tau_{FATIGUE} \approx \tau_{SR}$ for the range of loading frequencies employed.

(b) N_f depended critically on t_{max} (loading frequency). For instance, the mean value of N_f was increased by a factor of approximately 23 as the frequency increased from 0.86 to 6 cpm.

(c) The measured values of N_f agree well with those calculated from Equation 5.

The above points taken together indicate that the cumulative damage model can be applied to identify the number of loading cycles required to cause failure under fatigue. Thus the decreasing number of cycles to failure with decreasing frequency simply reflects the increased value of t_{max}. The significant damage and brittle crack propa-

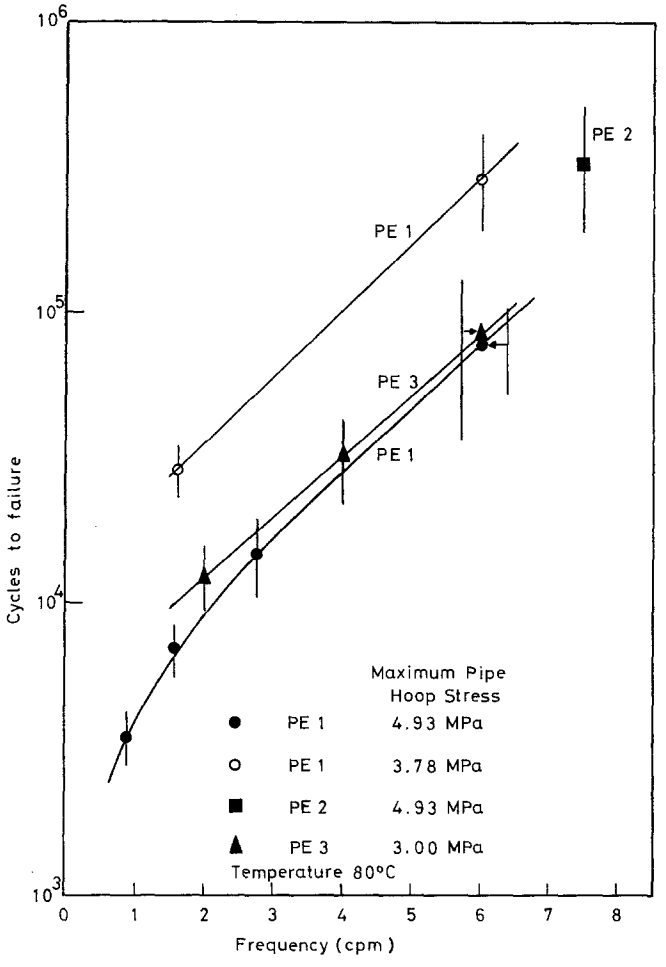

Figure 7 Number of cycles to failure, N_f, as a function of frequency of internal pressure loading. Note, frequency was varied only by varying the time under maximum load.

gation, from the initiating defect, then occurred during that section of the loading cycle when the pressure, and stress, were acting. Application of the "Paris Law", Equation 6, would be of very limited value.

For the PE3 pipes and the lower pressure tested PE1 pipes, the experimental and calculated values for N_f begin to differ, Fig. 13. Concomitant with the changes in N_f was the increased divergence between τ_{SR} and $\tau_{FATIGUE}$ as the frequency was increased, Fig. 5. This implies a deviation in behaviour from the cumulative damage model. This may be accounted for by proposing that at these lower stresses cracks propagated by a mixed mode, with both the application of the stress (Equation 6) and the time for which the stress acted (Equation 1) contributing significantly to crack growth. At high frequencies of loading it would be the application of the stress which would introduce most damage. Since B and b (Equation 1) and D and d (Equation 6) are material constants, and not necessarily equal, then the divergence between τ_{SR} and $\tau_{FATIGUE}$ for the PE3 and PE1 pipes at the lower stresses and higher frequencies may be accounted for. It would be expected, however, that $\tau_{FATIGUE}$ would tend towards τ_{SR} at the lower frequencies, as indeed it did, as the cumulative damage mechanism of crack propagation exerted the major effect.

However, it should be noted that at the lower stresses, and for the PE1 pipes in particular, the testing times (τ_{TEST}) increased markedly with increasing frequency, Fig. 6. The peak melting temperature and the crystallinity (from the area under the endotherm melting curve but neglecting the effect of additives) of these pipe materials were determined [22], and both changed during the course of a test, Figs. 14 and 15. In addition, the application of stress accelerated this change. Therefore, since measureable, and possible significant changes in the structure of the material occurred between 10 and 100 h at 80° C, the lower stress tested material may have been essentially

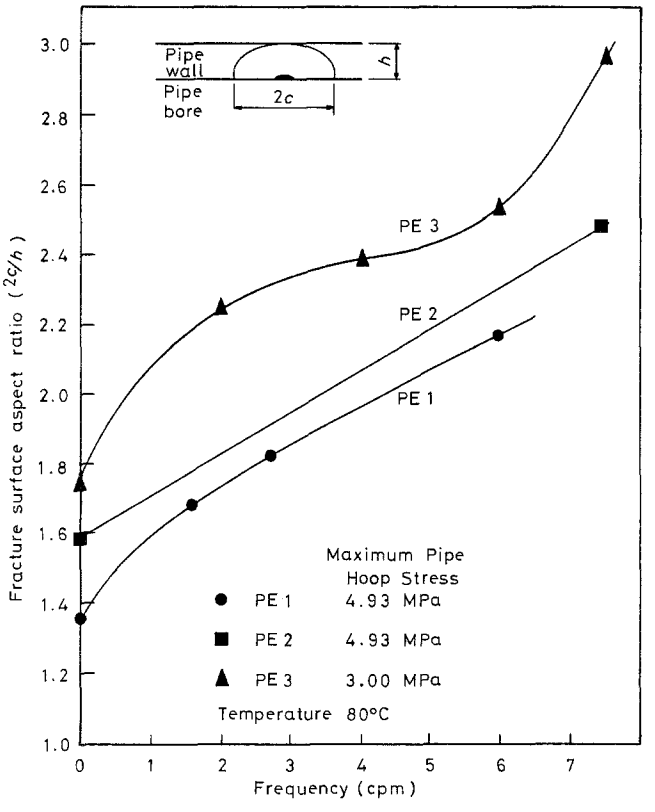

Figure 8 The aspect ratio of the fracture surface from the various pipes as a function of loading frequency. Each point is the result of measurements of the fracture surfaces of several pipes tested under the same conditions.

different from the higher stress tested PE1 pipe, and this may account for the divergence between $\tau_{FATIGUE}$ and τ_{SR}.

6.1.2. The fatigue performance of the PE2 pipes

The response of the PE2 pipes to fatigue was completely different from that of the PE1 and PE3 pipes. τ_{SR} and $\tau_{FATIGUE}$ differed markedly, Fig. 5, so that, for individual pipes, the ratio of $\tau_{FATIGUE}/\bar{\tau}_{SR}$ ranged from 0.06 to 0.18. In addition, the reduction in performance of the PE2 pipes under fatigue was such that all values for $\tau_{FATIGUE}$, when plotted onto the material manufacturer's stress-rupture curve, fell markedly to the left. The same did not apply to the PE1 and PE3 pipes loaded under fatigue.

The behaviour of the PE2 pipes under fatigue cannot reasonably be described by a cumulative damage model. Using the measured value of $\bar{\tau}_{SR}$

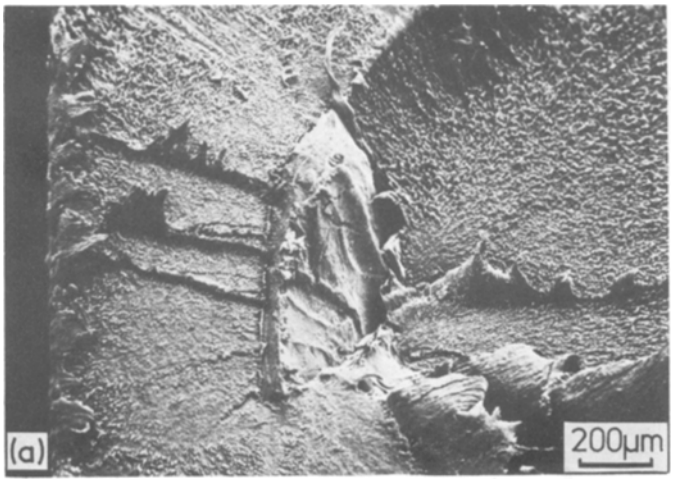

Figure 9 Scanning electron micrographs from selected failed PE1 pipes highlighting the particles at the source of fracture initiation. (a) and (b) are fracture initiating particles in which, on EDX analysis, no elements were detected, (c) is a calcium rich particle and (d) an iron based particle (see Fig. 11).

Figure 9 Continued.

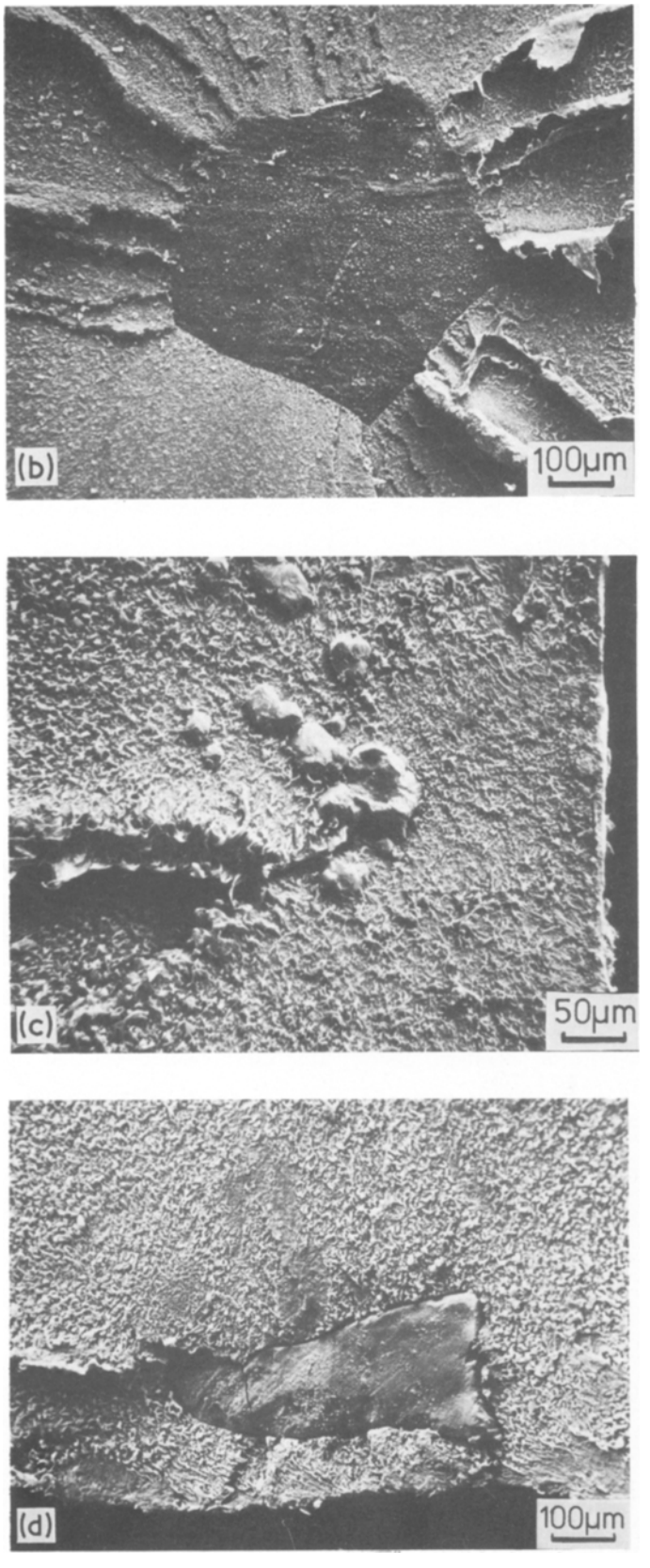

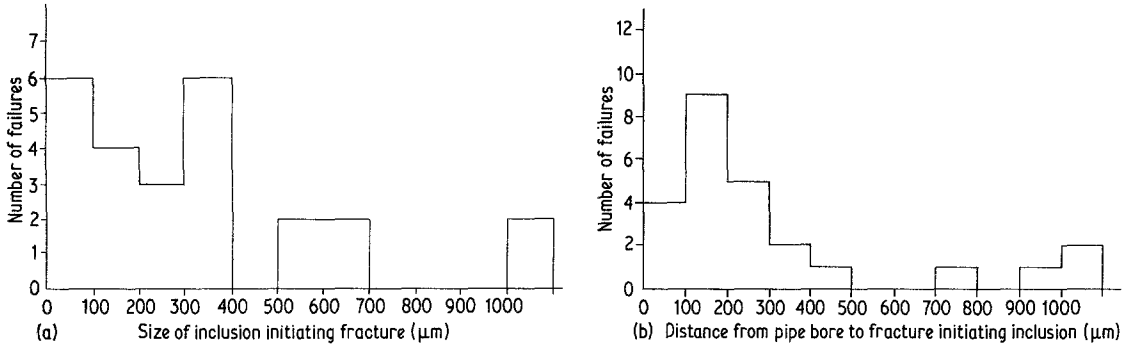

Figure 10 Histograms of the fracture initiating particle size (a) and position of the centre of the particle from the pipe wall (b). These relate only to the failure of the PE1 pipe and include both stress-rupture and fatigue tested pipe.

and Equation 5, the value of the calculated number of cycles to failure is of the order of 3×10^6, whereas for certain individual pipes N_f was less than 2×10^5. These polyethylene pipes thus exhibited a clear fatigue weakness. Previous investigations into the response of polyethylene pipes to fatigue or "intermittant creep" loadings found no weakness. However, the study of Lortsch [26] used testing conditions (stress and temperature) that would produce, under constant pressure, a ductile failure. Work by ourselves has indicated that if a pipe system, containing a known weakness under fatigue, is tested in both the ductile and brittle regions of the stress-rupture curve, then only those conditions that would produce a brittle fracture will cause the fatigue weakness to be made apparent. Therefore, the results of the work of Lortsch are not surprising, in that no fatigue

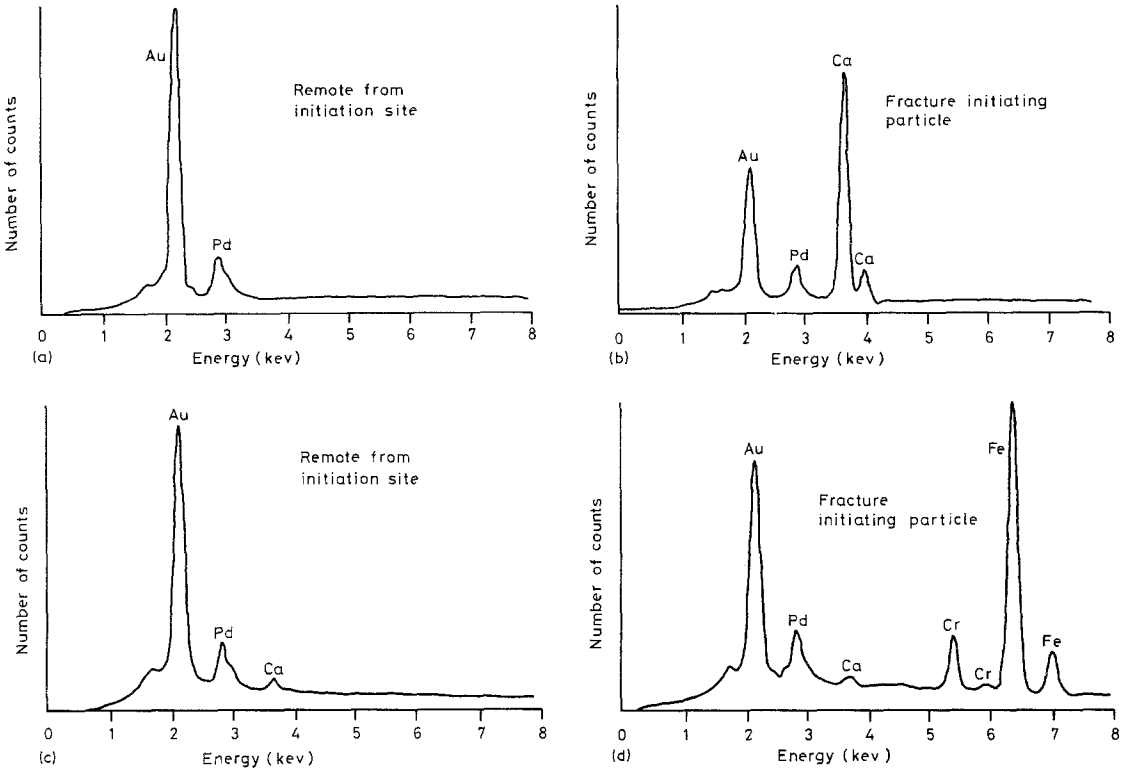

Figure 11 EDX spectra from the fracture initiating particle and remote from the initiation site for calcium rich ((a) and (b)) and iron based ((c) and (d)) particles. The lines for gold and palladium are from the coating process. The spectra for those particles in which no elements were detected are identical with the spectra remote from the initiation site.

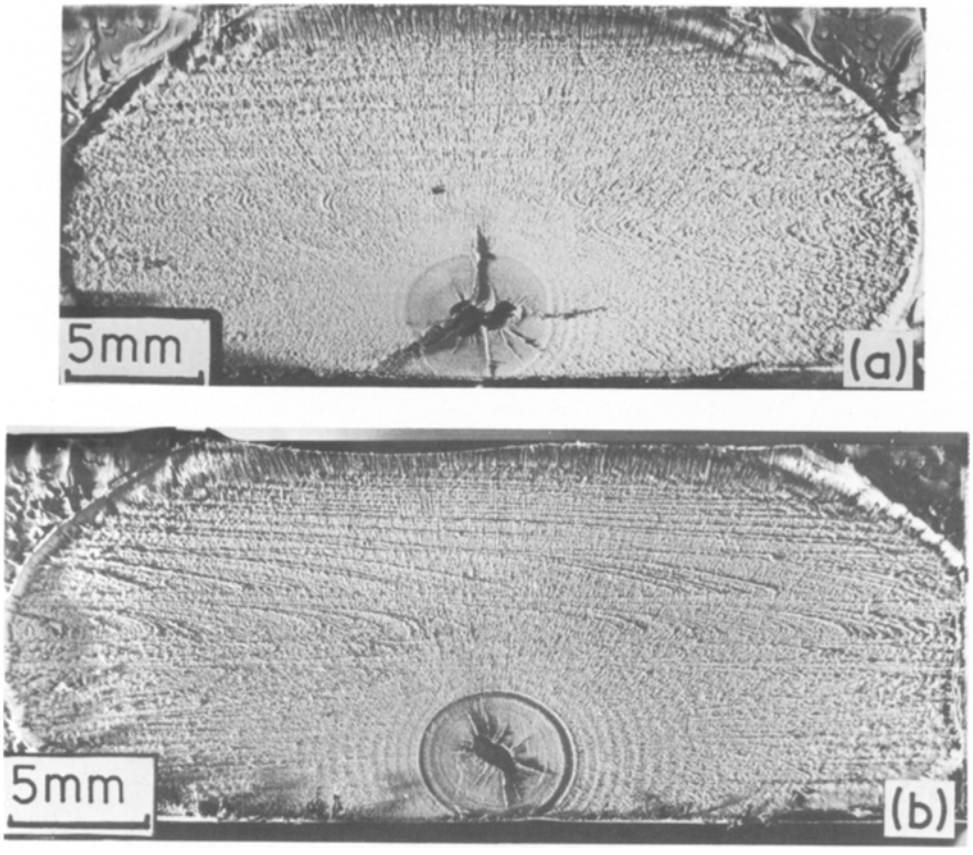

Figure 12 (a) and (b) Low magnification optical photomicrographs of fracture surfaces of the large diameter pipe when failure initiated from large voids. In all cases these lay close to the bore of the pipe.

weakness was identified. In the other study on the response of polyethylene (HDPE) pipes to fatigue, the combination of the testing temperature (20° C) and maximum hoop stress (17.5 to 21 MPa) would give rise to ductile failure [27]. The system lifetime, τ_{FATIGUE}, calculated approximately from the value of N_f, showed no weakness, as would be expected, from the statement above.

Eleven fatigue tests and ten failures were recorded in the PE2 pipes, to confirm that a polyethylene pipe could exhibit a fatigue weakness. This relatively large number of tests also allowed an examination to be made of the most appropriate distribution of lifetimes. The best distribution was a three parameter Weibull distribution, with lifetime expressed as $(\tau_{\text{FATIGUE}} - \mu)$, where $\mu = 51.6$ h [28].

The cause of the premature failure of the fatigue loaded PE2 pipes was either by a true fatigue failure, or due to a tendency for the crack growth to start early in fatigue, or to some combination of these effects. Crazed or damaged material is known to exist ahead of a crack [15, 20, 29]. The action of fatigue unloading may lead to the collapse and buckling of this material. On reloading the ability of the crazed material to resist crack growth is reduced, hence the increased rate of crack growth under fatigue or intermittant loading [20]. Increasing the regularity of the collapsing and buckling of material then accelerates crack growth [20]. With this mode of failure Equation 6 defines crack growth rates, which are in terms of da/dn, so that the number of cycles to failure, N_f, should change little with changes in t_{max} (assuming t_{max} stays within reasonable limits).

Turning to the possibility of crack growth starting early in fatigue, there is some evidence for this from an examination of the fracture surfaces. The site of fracture initiation under fatigue and stress-rupture testing differed for the PE2 pipes; the fatigue fractures initiated in the highest stressed region, near the pipe bore (see Appendix), while under constant pressure the cracks often

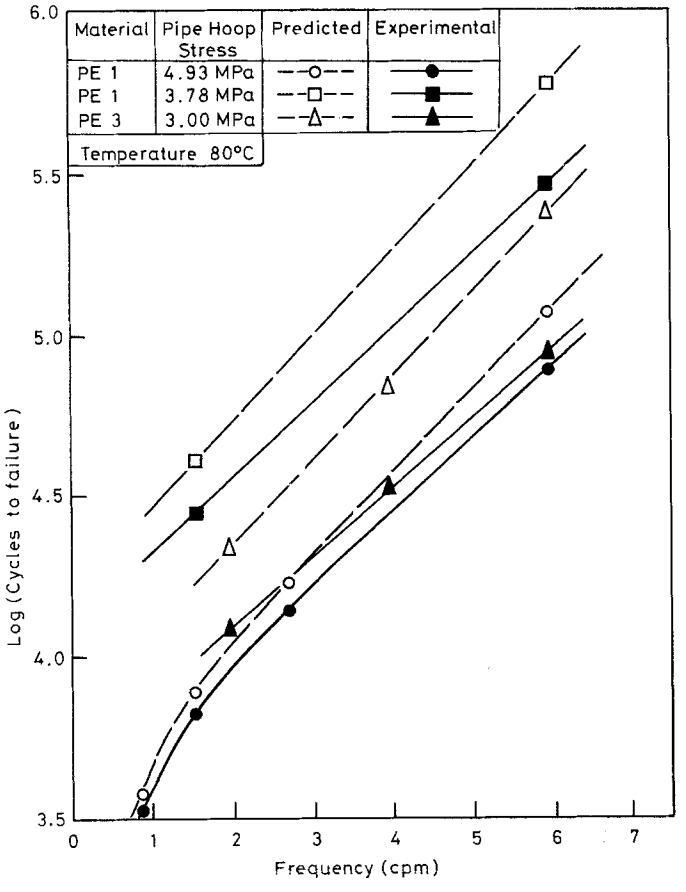

Figure 13 A comparison of the recorded and predicted (according to Equation 5 and the measured stress-rupture lifetime) number of cycles to failure for the three pipe tests as a function of loading frequency.

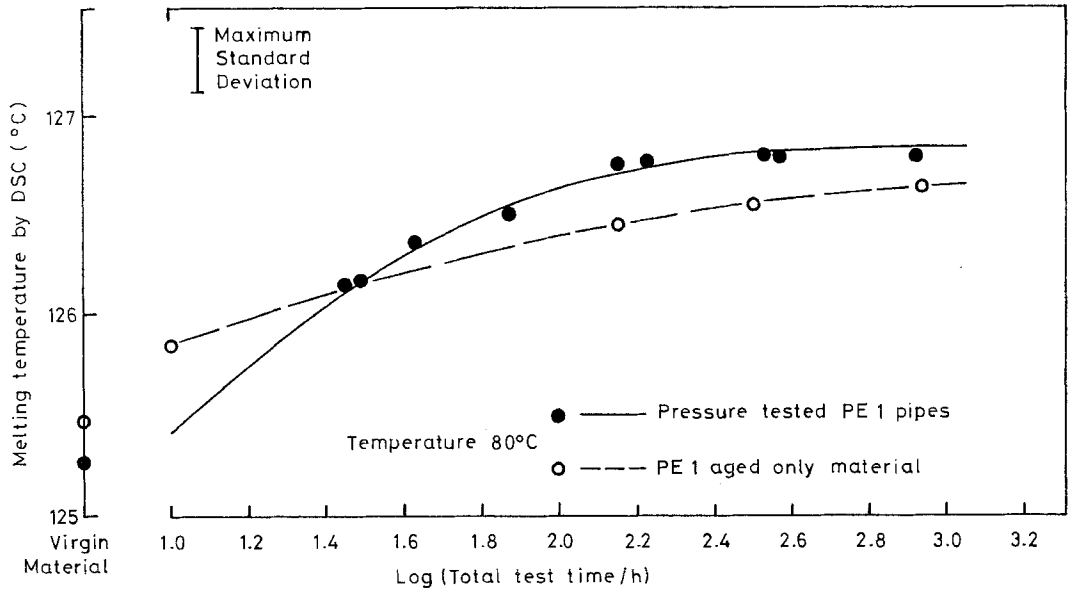

Figure 14 For samples of material cut consistently from the centre of PE1 pipes, the influence of time in a water bath at 80° C on the material melting temperature. The solid curve relates to material taken from close to the fracture surface of failed pipes which had been subjected to stress due to internal pressurization, the broken curve to samples simply suspended in the tank. Sample size about 5 mg, heating rate 10 K min^{-1}, sensitivity 5 $mcal^{-1}$ using a Perkin–Elmer

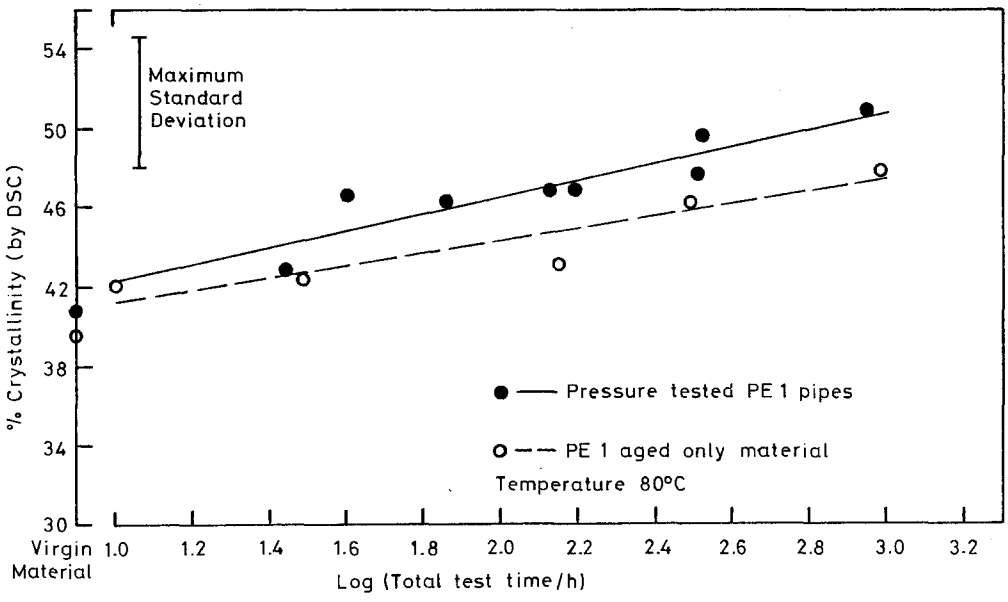

Figure 15 The influence of stress and time in a water bath at 80° C on the DSC measured crystallinity. See Fig. 14 for testing conditions and legend. The value for the enthalpy of fusion of polyethylene was taken as 286 kJ kg^{-1}.

initiated near the centre of the pipe wall, see Fig. 4. Since pipes have internal stresses from processing, and these exaggerate the difference between the bore and outside wall stress [30] to further favour fracture initiation at or near the pipe bore, then the initiation of the brittle fractures from particles at or towards the centre of the pipe wall, when testing under constant pressure, supports the notion that crack growth was delayed until the internal stresses were reduced by annealing. The short lifetime of the fatigue tested pipe may then be simply put down to early crack propagation.

6.2. Macro-features of the fracture surfaces of the small diameter pipes

Figs. 4 and 8 show that for all the small diameter polyethylene pipes tested, the overall shape of the brittle fracture surface was characteristic of the imposed loading mode. Stress-rupture testing gave rise to a fracture surface which was nearly symmetrical about the middle of the pipe wall, and similar in shape to those previously reported [7, 8]. Under fatigue the crack propagated preferentially along the pipe bore. This shape is similar to that observed for fatigue failures in uPVC (unplasticized poly(vinylchloride)) pipe [21]; there is no readily available evidence for fracture surface shapes in fatigue loaded polyethylene pipe. The preferential pinning of the crack at the pipe bore, when loaded under constant pressure, may be related to changes from plane stress to plane strain in going from the pipe bore to the middle of the pipe wall [31]. Such pinning did not occur under fatigue, Fig. 4. This preferential growth of the crack along the pipe bore occurred with the fatigue weak PE2 pipes and the more fatigue resistant PE1 and PE3 pipes. Therefore, it is not related to the material but is a function of the loading mode. From the large (160 mm) diameter thick (14.5 mm) walled pipe that was fatigue tested, the fracture surface shape was similar to the fatigue tested small diameter pipe.

The change in fracture shape when going from stress-rupture to fatigue loading has two possible consequences. First, the fracture surface of a failed polyethylene pipe may aid in identifying the loading mode that caused fracture. All three small diameter pipes (PE1, PE2 and PE3) displayed the same change in fracture surface shape with change in loading mode. In addition other polyethylene resins and pipe sizes, tested but not reported here, displayed a similar trend. Secondly, the stress intensification at the tip of a growing crack is a (complex) function of many variables. Following Irwin [32], the influence of the shape of the crack, in terms of depth to length, on the stress intensification has been widely recognised

[33, 34]. As the crack shape changes from semicircular (the ratio of the crack depth to the crack length, along the pipe, is equal to 0.5) to that characteristic of fatigue (the above ratio is less than 0.5), with this change the stress intensification is greater, and therefore the lifetimes of pipes having elongated fracture surfaces should be less than the semicircular. This may, in part, account for the small reduction in performance of the PE1 and PE3 pipes loaded under fatigue.

If, however, crack shape is to influence lifetime, the differences in shape observed after final rupture of the pipe must also be present as the crack grows. Evidence from some part ruptured fatigue and stress-rupture tested pipe, and discontinuous crack growth bands on some fatigue failed pipe, Fig. 4, support the contention that for significant fractions of the total wall thickness of the pipe, the fracture surface shape of the growing crack was characteristic of the loading profile. It must be noted, however, that the greatest fraction of the lifetime is spent when the crack is small, the region where there is little information on the shape of the growing crack. Further there was no evidence that the particles initiating fracture in the fatigue tested pipe were different in position, size or shape from those found in the stress-rupture tested pipe. Therefore, the initial shape of the growing fractures must be similar under both loading modes, so that the fracture surface shape may not have a major influence on pipe lifetime as data in Fig. 5 shows for the PE1 and PE3 pipe materials.

6.3. The initiation of the brittle fracture of polyethylene pipes

6.3.1. The influence of particle size on the lifetimes of the PE1 pipes

Fig. 9 clearly shows that brittle fractures in fatigue and stress-rupture tested PE1 polyethylene pipes were initiated at particles. Figs. 10a and b show, respectively, that there was a range of particle sizes and positions, with respect to the inside wall of pipe. In Section 3.2 it was indicated, Equation 4, that the size of the particle initiating fracture controlled the lifetime of plastics pipes, assuming crack growth is described by an equation of the form as Equation 1. A correlation, therefore, was sought between the size of the particle initiating fracture and a measure of the lifetime of the pipe. Since only a limited number of stress-rupture tests were undertaken, the data from the fatigue tests was incorporated. In Section 6.1.1 the performance of the PE1 pipes under fatigue was shown to be described by the cumulative damage model, allowing the incorporation of this data with the stress-rupture data. However, there was a small fall-off in performance with increasing frequency for the PE1 pipes, see Fig. 5. To allow for this fall-off, the lifetime of a given pipe is expressed in relation to the mean lifetime of that test (conducted at a given pressure, and with the same loading form and frequency) of which it was a part: thus, as $\tau/\bar{\tau}$, where $\bar{\tau}$ is the mean lifetime of the group of the pipe samples of which τ is the lifetime of one, and $\tau/\bar{\tau}$ is known as the reduced lifetime.

Various plots were made of reduced lifetime against the size of the inclusions leading to fracture, (a_0), using different measures of particle dimensions (for example, maximum size, extent of the particle along and perpendicular to the pipe axis, etc.). The best fit was obtained on a log $(\tau/\bar{\tau})$ against log (a_0) plot, where a_0 is the maximum inclusion size in the plane of the fracture surface irrespective of direction. The data is presented in Fig. 16 where the sample size of 22 gave a correlation coefficient of -0.49. The preferred log $(\tau/\bar{\tau})$ against log (a_0) relationship infers that the measured individual lifetimes of the PE1 pipes can best be predicted by using the fracture mechanics approach as proposed by Gray and co-workers [5, 12], with the lifetimes, τ_{FATIGUE}, of the fatigue tested PE1 pipes included as they failed according to cumulative damage principles. The negative correlation coefficient confirms the dependence of pipe lifetime on initiating particle size as described by Equations 3 and 4, increasing initiating particle size reducing pipe lifetime. In addition, particle size was predominantly within the range 200 to 1000 μm, which for a pipe hoop stress of 4.93 MPa gave values for K_c (0.14 to 0.31 $\text{MN m}^{-3/2}$) for which measurable crack growth occurs for similar polyethylenes [5].

The log $(\tau/\bar{\tau})$ against log (a_0) plot of Fig. 16 allows the constant b (see Equation 1) to be calculated from the slope of the curve; the value comes out at approximately 2.36, close to values recorded by Gray and co-workers [12, 35] on similar polyethylene materials from crack propagation studies. However, if the value for h, typical values of a_0, and the approximate value for b from Fig. 16 are inserted into the square brackets of Equation 3, the approximation

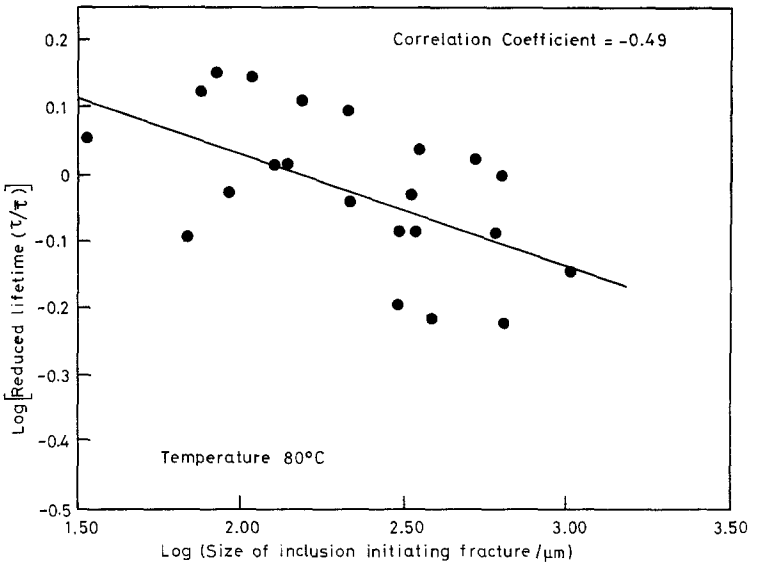

Figure 16 A double logarithmic plot of reduced lifetime against the size of the particle initiating fracture. This data was obtained from stress-rupture and fatigue testing the PE1 pipes at 80° C.

$$a_0^{(1-b/2)} - h^{(1-b/2)} \simeq a_0^{(1-b/2)} \qquad (10)$$

does not hold. The use of Equation 4 to describe the influence of initiating particle size on pipe lifetime is therefore approximate for values of b close to 2 with the size of defects observed in this study. An equation of the form of 3 must be used. However, both Equations 3 and 4, and the data in Fig. 16, indicate that for these PE1 pipes, lifetime will depend upon the size and concentration of included defects. A similar lifetime–particle size relationship may not apply to other polyethylene pipe materials.

One difference exists between our work and the calculations of Gray, Mallinson and Price on the fracture of polyethylene pipe; the size of the particles initiating fracture. In the calculations of Gray *et al.* [12], the particle size was calculated to be within the range 10 to 100 μm, whereas this present work (see Fig. 10) found the particles to be considerably larger, in the range 100 to 600 μm. The difference may be due to either a delay in the start of crack growth, an incubation period, or in the value of the geometrical parameter Y (see Equation 2). Gray *et al.* assumed the shape of the growing crack to be semi-elliptical [35]. Figs. 4a, b and c and [7] and [8], show that for stress-ruptured small diameter pipe, this is not the case. If Y had a smaller value, or there was an incubation period, then the particle size required to initiate fracture may have to be put at a higher value and the difference may be accounted for.

6.3.2. The nature and origin of initiating particles

Three major types of particles were identified; particles where no elements were detected, iron based particles and calcium rich particles. The impurities associated with base polymer production and compounding were largely accounted for by the calcium rich particles, presumed to be calcium stearate, and high molecular weight polymer or gels for which no elements were detectable by the EDX technique. The particles associated with pipe manufacture were the iron based particles, including 316 stainless steel, and were associated with plastics processing equipment wear or damage. The fibrous impurities arose from materials handling including the packaging of the feedstock. An example of a fibrous inclusion initiating fracture is shown in Fig. 17.

Methods for improving the performance of polyethylene pipes may, therefore, be directed to either, or both, a reduction in the size and concentration of defects likely to initiate fracture, or to improving the material by either slowing down the rate, or delaying the start, of crack growth. The former route is the more straightforward, and for a given pipe material the reduction of the size and concentration of defects in the pipe wall can be realized by the informed use of currently available melt filtration units at the compounding or profile extrusion stages of manufacture [36, 37]. Filtration to 50 μm particle size should be realizable for pipe applications and

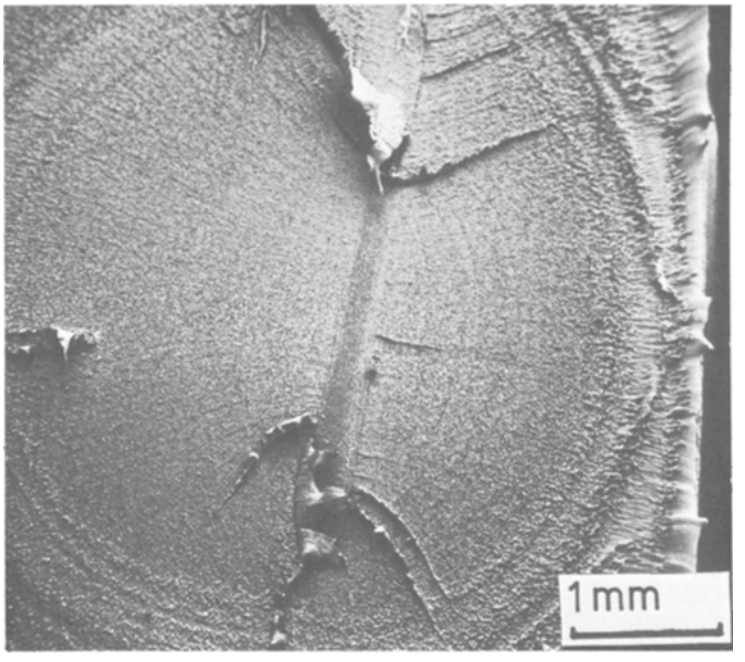

Figure 17 Fibrous inclusion which initiated the fracture of a fatigue tested PE1 pipe. Note that when fracture is initiated by such an inclusion the aspect ratio of the fracture surface does not conform to that predicted by Fig. 8.

would lead to improvements in the performance of certain, if not all, polyethylene pipes. If the plastics material obeys a crack growth relationship of the form of Equation 1 (for stress-rupture testing) or Equation 6 (for fatigue testing), then reducing the size of particles within the pipe wall will, as Equation 4 and Fig. 16 indicate, improve the performance of the pipe.

6.4. Fatigue behaviour of the large diameter thick walled pipes

160 mm outside diameter SDR11 pipe, produced from the PE1 material, contained massive voids in the wall of the pipe, Fig. 12. The voids gave rise to a major intensification of stress, so that fracture would be expected to initiate from the voids. Failure progressed from such voids and seriously weakened the pipe, reducing performance by, typically, an order of magnitude.

For some pipes produced in the United Kingdom and used for the distribution of gas, this possibility of voiding has been appreciated and anticipated. Ultrasonic techniques, primarily developed for wall thickness control, may also be used to identify if voids are present [38]. Thus non-destructive techniques are available to identify such defects, so that void-free polyethylene pipe can be produced and can be shown to be so.

The origin of the voiding in pipe is associated with two effects. First, in the production of pipe rapid cooling from the outside can cause considerable stresses to be frozen into the pipe. The general distribution of the stresses is such that the outside of the pipe is in compression, while close to the pipe bore the material suffers a tensile stress [30]. This may give rise to voiding [39]. Secondly, polyethylene materials shrink substantially in going from the liquid to the solid phase [40]. If the bore and outside of a pipe are first cooled, then the material in towards the middle of the pipe, being at a higher temperature and therefore lower modulus, cannot deform the lower temperature material either side to compensate for the shrinkage. Voiding is then the result. Clearly, both shrinkage and internal stresses may operate together to create voiding.

Voiding is, therefore, more likely to occur with the higher density polyethylene materials, which, having a high crystallinity, will shrink to a greater extent than a medium density material. Secondly, control of processing conditions, including the temperature of the water bath, is also critical in determining whether voiding is present.

7. Conclusions

In the introduction three distinct areas of work were identified. The conclusions from the work undertaken on these three areas are:

(a) Small diameter polyethylene pipes subjected to a fluctuating internal pressure loading

may or may not exhibit a fatigue weakness. The tendency towards a fatigue weakness is material specific. For those materials not exhibiting a major fatigue weakness the number of cycles to failure, N_f, may be indicated using the stress-rupture lifetime, τ_{SR}, and the time under maximum load, as indicated by Equation 5 from Stapel [17, 18].

Pipes exhibiting a fatigue weakness have a low value of $\tau_{FATIGUE}/\bar{\tau}_{SR}$, and in some cases $\tau_{FATIGUE}$ may lie to the left of the material manufacturer's stress-rupture curve. However, τ_{TEST} may be equal to or greater than $\bar{\tau}_{SR}$, due to the time off-load. In this case the user of the pipe will not notice any weakness in fatigue. It is our opinion that the ratio of $\tau_{FATIGUE}/\bar{\tau}_{SR}$ must be lower than that recorded for the PE2 pipe for a fatigue weakness to become apparent for pipes used in the field. This is provided that the user of the pipe is aware of the maximum pulse pressure, which may differ from the static case. Design must then centre on the highest stress. These comments may not apply if the pipe is poorly processed or badly installed.

(b) Fig. 16 established that the presence of large included particles in pipe reduced pipe performance. The data presented in the figure relates to one relatively short lifetime pipe material. The same conclusions may not apply to other pipe materials, particularly if there is a substantial incubation period prior to crack growth. However, for polyethylene pipe materials similar to the PE1, pipe performance may be improved by filtration of the melt, at the pipe extrusion stage, to reduce the size and concentration of defects. An analysis of uPVC pipe failures by Kirby [41] highlighted included particles as a major cause of premature pipe failure, accounting for in excess of 11% of the 300+ failures examined. This field experience with uPVC then agrees with our laboratory studies with the PE1 pipe.

The presence of particles, such as those identified in Figs. 9, 10 and 11, can be traced to several sources, including base polymer manufacture, materials handling, including the container used, and to defects introduced during processing. Attention must be directed to all stages of the production of a finished article if performance is to be enhanced. We would expect included particles to affect the performance of other profiles and injection moulded artefacts.

(c) Thick walled large bore pipe is more expensive and difficult to test. However, it is evident that problems exist with large bore pipe which are not found in the smaller diameters. This relates particularly to the possibility of large (mm in dimensions) voids forming in the wall of the pipe. There is no information to hand to suggest that such defects would not reduce stress-rupture lifetimes as well as $\tau_{FATIGUE}$. Care must be taken in the processing of large diameter pipes to avoid such problems. Tests have been conducted on other thick walled (125 mm SDR11 and 180 mm SDR17) polyethylene pipe with no evidence of substantial fatigue weaknesses arising from voiding in the wall of the pipe.

Finally, we conclude this paper with the following general points:

(i) All three small diameter polyethylene pipes were within the material manufacturer's specification, both in terms of the material melt index, density and melting temperature, and in the measured stress-rupture lifetime, short-term burst strength and material tensile strength (the last two properties were determined but are not recorded here).

(ii) The existing specifications and standards for polyethylene pipe seldom take into account the possibility of cyclic internal pressure loading. Published data [21, 24] for uPVC pipes clearly indicate that thermoplastic pipe materials can exhibit a weakness under fatigue, so that the uPVC pipe is down-rated if it is to be subjected to fatigue [42]. These present results, and more recent but incomplete data obtained within our laboratories on polyethylene pipe, indicate the possibility of a fatigue weakness in polyethylene pipe materials. For certain uses of pipe new standards, incorporating a fatigue test, may be desirable.

(iii) The weaknesses identified to date in polyethylene pipe are not dramatic ($\bar{\tau}_{FATIGUE}$ is, at worst, half the material manufacturer's specified stress-rupture lifetime for that temperature and hoop stress). However, the authors and others have already indicated, by presenting some preliminary results [43, 44], the possibility of severe weaknesses arising in certain polyethylene pipeline systems when loaded under fatigue. Failure occurs in the injection moulded fitting and the ratio of $\bar{\tau}_{FATIGUE}/\bar{\tau}_{SR}$ may be of the order of 0.005, so that system performance is reduced by in excess of two decades (using the material manufacturer's stress-rupture data). These results on the influence of injection moulded fittings on pipe system performance are to be presented in future publications [3].

Acknowledgements

The authors wish to acknowledge the financial support of the Polymer Engineering Directorate of the Science and Engineering Research Council and the provision of materials and welding facilities by Corrosion Resistant plastics Ltd. The authors are indebted to Mr S. R. Bentley for his practical contributions to the work presented in this paper, and to the following for valuable discussions; Mr W. E. Cowley (Associated Octel Co. Ltd), Dr R. Roberts (ICI PLC), Dr A. Gray (BP Chemicals Ltd) and Dr P. Leevers (Imperial College, London University).

Appendix

The hoop stress in the pipe (σ_H) is calculated using "Barlow's formula"

$$\sigma_H = \frac{P_i(d_{OD} - h)}{2h} \qquad \text{(A1)}$$

where P_i is the internal gauge pressure, $(d_{OD} - h)$ the mean pipe diameter and h the wall thickness.

For SDR11 pipe, which is relatively thick walled, the pipe wall hoop stress varies with distance from the pipe axis (r) as

$$(\sigma_H)_r = \frac{P_i R_{ID}^2}{R_{OD}^2 - R_{ID}^2}\left[\frac{r^2 + R_{OD}^2}{r^2}\right] \qquad \text{(A2)}$$

where R_{ID} and R_{OD} are the internal and external pipe radii. For SDR11 pipe the ratio of the hoop stress at the pipe bore to hoop stress at the outside wall is approximately 1.25. Residual stresses can further exaggerate this difference.

References

1. E. GAUBE, G. DIEDRICH and W. MULLER, *Kunststoffe* **66**, (1976) 2.
2. P. C. KIRBY, *Plast. Rubber: Mater. Appl.* **5** (1980) 78.
3. M. BARKER, J. BOWMAN, S. BENTLEY and M. BEVIS, in preparation.
4. K. GOTHAM, *Plast. Polym.* Aug (1969) 309.
5. J. B. PRICE and A. GRAY, PRI 4th International Conference on Plastics Pipes, Brighton, England, March 1979 (Plastics and Rubber Institute, London).
6. "Designing with Plastics: Materials Under Stress", T351 12A (The Open University Press, Milton Keynes, England).
7. C. G. BRAGAW, *Plast. Rubber: Mater. Appl.* **4** (1979) 145.
8. L. ENGEL, H. KLINGELE, G. W. EHRENSTEIN and H. SCHAPER, "An Atlas of Polymer Damage: Surface Examination by SEM" (Wolfe Science Books, 1981).
9. J. G. WILLIAMS, "Stress Analysis of Polymers" 2nd edn (Ellis Horwood, Chichester, England, 1980).
10. B. D. COLEMAN, *J. Polym. Sci.* **20** (1956) 447.
11. S. J. BARTON and B. W. CHERRY, PRI 4th International Conference on Plastics Pipes, Brighton England, March 1979 (Plastics and Rubber Institute, London).
12. A. GRAY, J. N. MALLINSON and J. B. PRICE, *Plast. Rubber Process. Appl.* **1** (1981) 51.
13. J. M. SCHULTZ, in "Properties of Solid Polymeric Materials, Part B, Treatise on Materials Science and Technology" edited by J. M. Schultz (Academic Press, New York, 1977) p. 599.
14. J. A. MANSON and R. W. HERTZBERG, *Crit. Rev. Macromol. Sci.* **1** (1973) 433.
15. R. W. HERTZBERG and J.A. MANSON, "Fatigue of Engineering Plastic" (Academic Press, New York, 1980).
16. G. B. McKENNA and R. W. PENN, *Polymer* **21** (1980) 213.
17. J. J. STAPEL, *Pipes Pipeline Int.* **22** (1977) 11.
18. *Idem ibid.* **22** (1977) 33.
19. J. C. RADON, S. ARAD and L. E. CULVER, *Eng. Fract. Mech.* **6** (1974) 195.
20. F. X. de CHARENTENAY, F. LAGHOUATI and J. DEWAS, PRI 4th International Conference on Deformation, Yield and Fracture of Polymers, Cambridge, England, April 1979 (Plastics and Rubber Institute, London).
21. S. H. JOSEPH, PRI 4th International Conference on Plastics Pipes, Brighton, England 1979.
22. M. B. BARKER, PhD Thesis, Brunel University (1982).
23. G. FORD, M. B. BARKER, K. W. BATCHELOR and J. BOWMAN, in preparation.
24. J. V. GOTHAM and M. K. HITCH, *Pipes Pipeline Int.* **20** (1975) 10.
25. H. H. KAUSCH, "Polymer Fracture. Polymers Properties and Applications" Vol. 2 (Springer-Verlag, New York, 1978).
26. W. LORTSCH, *Kunststoffe* **55** (1965) 460.
27. Hoechst Aktiengesellschaft, Frankfurt am Main, West Germany. Private communication (1979).
28. D. H. YOUNG, Brunel University, private communication (1981).
29. J. R. WHITE and J. W. TEH, *Polymer* **20** (1979) 764.
30. J. G. WILLIAMS, *Plast. Rubber Process. Appl.* **1** (1981) 369.
31. P. LEEVERS, Imperial College, London University, private communications (1982).
32. G. R. IRWIN, *Trans, ASME J. Appl. Mech.* **84E** (1962) 651.
33. W. G. CLARK, Jr, *Trans. ASME J. Eng. Ind.* **94** (1972) 291.
34. A. P. PARKER, "The Mechanics of Fracture and Fatigue" (Chapman & Hall, London, 1981).
35. A. GRAY, BP Chemicals Ltd., private communication (1982).
36. T. A. MURRAY, *Plast. Technol.* **23** (1977) 65.
37. M. BEVIS, in "Filtration of Polymer Melts" translated by M. S. Welling (Verein Deutscher Ingenieure VDI-Gesellschaft Kunstofftechnik, VDI-Verlag, Dusselforf, 1981).

38. M. G. LOFTHOUSE, at Short Course on Plastics Pipes, Brunel University, 1980.
39. G. PITMAN, Proceedings of 2nd Short Course on Plastics Pipes, Brunel University, Uxbridge, UK, September 1981.
40. A. B. GLANVILLE, from "Thermoplastics: Effects of Processing" edited by Ogorkiewicz, (Plastics Institute, London, 1969).
41. P. C. KIRBY, from Proceedings of the International Conference on Underground Plastic Pipe, ASCE, New Orleans, USA, 1981.
42. D. R. MOORE, Proceedings of 2nd Short Course on Plastics Pipes, Brunel University, Uxbridge, UK, September 1981.
43. M. BARKER, J. BOWMAN, S. BENTLEY and M. BEVIS, PRI International Conference on Moulding of Polyolefins, London, England, November 1980 (Plastics and Rubber Institute, London).
44. W. E. COWLEY and L. E. WYLDE, *Chem. Ind.* (1978) 371.

Received 18 August
and accepted 2 September 1982